Modification of Spin Density Distribution via Specific Hydrogen Bond Interactions: An Experimental, UHF, and Density Functional Study

Angelika Niemz and Vincent M. Rotello*

Contribution from the Department of Chemistry, University of Massachusetts, Amherst, Massachusetts 01003

Received March 12, 1997. Revised Manuscript Received April 25, 1997[⊗]

Abstract: A combined experimental/computational study has been carried out on the effect of hydrogen bond complex formation between the radical anion of naphthalimide and the acylated diaminopyridine receptor **2**. Experimental hyperfine coupling constants (hfc's) were obtained via simultaneous electrochemistry and EPR (SEEPR). An overall increase in the absolute values of the hfc's is observed. To better correlate experimental results with changes in electronic structure, hfc's were calculated using UHF and UKS wave functions, specifically the B3LYP hybrid functional. While the UHF derived hfc's reproduce qualitative trends, the hfc's obtained by density functional calculations are in good quantitative agreement with the experimental data. B3LYP calculations show an increase in spin polarization, with the largest effect observed in the naphthyl moiety, consistent with experimental results.

Introduction

Alteration of the chemical and physical properties of radicals via hydrogen bonding has received widespread attention in recent years in the context of biochemistry, chemistry, and material science. The scope of this research extends from the generation of organic ferromagnets via propagation of spin coupling through hydrogen bonds[1−3] to the stabilization of biological radicals through interaction with the protein scaffolding (e.g., Qa in the bacterial photosynthetic reaction center,[4] tyrosyl radicals in photosystem II[5] and ribonucleotide reductase,[6] and flavin semiquinone radicals in flavoenzymes[7,8]).

Model systems allow the parametric study of the change in electronic structure of biologically significant radicals upon hydrogen bonding, providing insight into more complex enzymatic systems. Previously reported model systems have focused on nonspecific hydrogen bond interactions, e.g., between nitrobenzene radical anions and substituted acetylenes,[9−11] or the addition of protic solvent to the solution of ninhydrin radical anion in an aprotic medium.[12] In these systems, structural differences, the lack of specificity, and low association constants limit their ability to effectively mimic biological systems. Comparison between spectra acquired in a protic vs aprotic medium is also complicated by the change in the solvent dielectric. Additionally, quantitative evaluation of these model systems has for the most part relied on semiempirical relationships derived from Hückle and McLachlan theory,[13,14] introducing errors in the calculation of "experimental" spin densities from observed hyperfine coupling constants (hfc's).

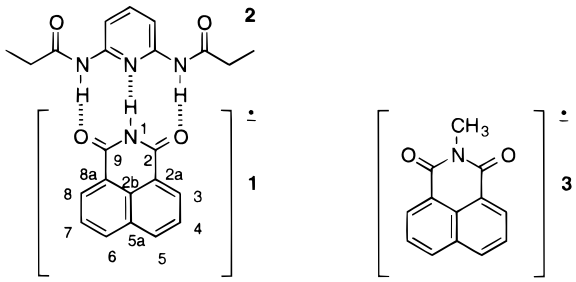

Figure 1. Hydrogen-bonded complex between naphthalimide radical anion **1** and receptor **2**, negative control *N*(1)-methylnaphthalimide **3**, in which the binding site is blocked via alkylation.

We here report the first model study in which the spin density distribution of a radical anion is modified through *specific* hydrogen bond interactions. The system studied is the complex formed between the naphthalimide anion radical **1** and the acylated 2,6-diaminopyridine receptor **2** (Figure 1).[15] Similar imide−diaminopyridine recognition has been previously utilized to mimic modification of flavin-cofactor redox chemistry through hydrogen bonding.[8] The naphthalimide **1**−receptor **2** complex is sophisticated enough to represent important features of more complex systems, yet simple enough to yield readily interpretable EPR spectra and allow the application of high-level computational methods.

[⊗] Abstract published in *Advance ACS Abstracts,* July, 1, 1997.

(1) Akita, T.; Mazaki, Y.; Kobayashi, K. *J. Chem. Soc., Chem. Commun.* **1995**, 1861.
(2) Sugawara, T.; Matsushita, M. M.; Izuoka, A.; Wada, N.; Takeda, N.; Ishikawa, M. *J. Chem. Soc., Chem. Commun.* **1994**, 1723−1724.
(3) Zhang, J. P.; Baumgarten, M. *Chem. Phys.* **1997**, *214*, 291−299.
(4) Bosch, M. K.; Gast, P.; Hoff, A. J.; Spoyalov, A. P.; Tsvetkov, Y. D. *Chem. Phys. Lett.* **1995**, *239*, 306−312.
(5) Tommos, C.; Tang, X. S.; Wrancke, K.; Hoganson, C. W.; Styring, S.; McCracken, J.; Diner, B. A.; Babcock, G. T. *J. Am. Chem. Soc.* **1995**, *117*, 10325−10335.
(6) Hoganson, C. W.; Sahlin, M.; Sjoeberg, B. M.; Babcock, G. T. *J. Am. Chem. Soc.* **1996**, *118*, 4672−4679.
(7) Edmondson, D. E.; Tollin, G. In *Topics in Current Chemistry*; Boschke, F. L., Ed.; Springer-Verlag: Berlin, 1983; Vol. 108; pp 109−138.
(8) Breinlinger, E.; Niemz, A.; Rotello, V. M. *J. Am. Chem. Soc.* **1995**, *117*, 5379−5380.
(9) Stevenson, G. R.; Echegoyen, L. *J. Am. Chem. Soc.* **1974**, *96*, 3381−3385.
(10) Stevenson, G. R.; Fraticelli, Y.; Concepcion, R. *J. Am. Chem. Soc.* **1976**, *98*, 3410−3414.
(11) Stevenson, G. R.; Castillo, C. A. *J. Am. Chem. Soc.* **1976**, *98*, 7950−7954.
(12) Reiter, R. C.; Stevenson, G. R.; Wang, Z. Y. *J. Phys. Chem.* **1990**, *94*, 5717−5720.
(13) McConnell, H. M.; Chesnut, D. B. *J. Chem. Phys.* **1958**, *28*, 107−117.
(14) Karplus, M.; Fraenkel, G. *J. Chem. Phys.* **1961**, *35*, 1312−1323.
(15) Ge, Y.; Lilienthal, R. R.; Smith, D. K. *J. Am. Chem. Soc.* **1996**, *118*, 3976−3977.

S0002-7863(97)00801-9 CCC: $14.00

Experimental Section

Materials and General Methods. Solutions were prepared using reagent grade CH_2Cl_2 dried via distillation over CaH_2. Tetrabutylammonium perchlorate (TBAP, obtained from SACHEM, electrometric grade) was recrystalized twice from water and dried for several days under high vacuum. Naphthalimide (obtained from Aldrich Chemical Co.) was recrystallized from CH_2Cl_2 and dried under high vacuum. Other chemicals were reagent grade, were obtained from Aldrich, and were used without further purification. *N*(1)-Methylnaphthalimide was obtained via methylation of naphthalimide (MeI, Na_2CO_3, DMF), according to literature procedures.[16]

Simultaneous Electrochemistry and EPR. Due to the lossy nature of the samples and to minimize perturbation of the microwave field by the working electrode, SEEPR experiments were carried out in a quartz flat cell.[16] A second glass part containing three ACE no. 7 threaded joints sealed via Teflon ferrules to hold the electrodes and a septum-capped ground glass joint for degassing and sample injection was connected to the top of the cell. The working electrode, a platinum gauze electrode, was inserted into the flat part of the cell. The Ag-wire pseudoreference electrode was positioned directly above the working electrode in order to minimize the iR-drop, and the auxiliary electrode, a platium wire spiral of large surface area, occupied the solvent reservoir above the flat section. The electrode leads were insulated via Teflon heat shrink tubing. After each experiment the working electrode was cleaned in concentrated HNO_3.

EPR spectra were recorded on an IBM ESP 300 X-band spectrometer equipped with a TE_{104} dual cavity. Naphthalimide solutions (10^{-3} M in CH_2Cl_2, 0.1 M TBAP) were degassed by bubbling argon through them for 5 min and then injected into the cell, which was previously flushed with argon. The cell was mounted within the spectrometer using custom-manufactured cell holders, which allow for precise alignment of the cell within the cavity in order to maximize the Q-factor. Bulk electrolysis was carried out simultaneous to signal acquisition (25 kHz field modulation, modulation amplitude 0.0475 G). Hyperfine coupling constants (hfc's) were determined through spectrum simulation and iterative curve-fitting using the software package WinSim from NIEHS.[17] Excellent correlation (correlation coefficient greater than 0.99) was achieved in most cases.

Calculations. UHF and DFT-B3LYP calculations were performed using the Gaussian 94 suite of programs on Silicon Graphics workstations.[18] UHF geometry optimization at the 3-21G level was followed by UHF and B3LYP 6-31G* single point calculations. Isotropic hfc's were calculated according to

$$a(\mathrm{N}) = (8\pi/3)g_e\beta_e g_N\beta_N\rho(r_N)$$

The hfc of nucleus N, a(N), is proportional to the corresponding Fermi contact integral (spin density at the nucleus) $\rho(r_N)$; g_e (g_N) stands for the electronic (nuclear) g-factor and β_e (β_N) for the Bohr (nuclear) magneton.[19]

Results and Discussion

The EPR spectrum of the naphthalimide radical anion **1** was altered significantly by the addition of receptor **2** (Figure 2).

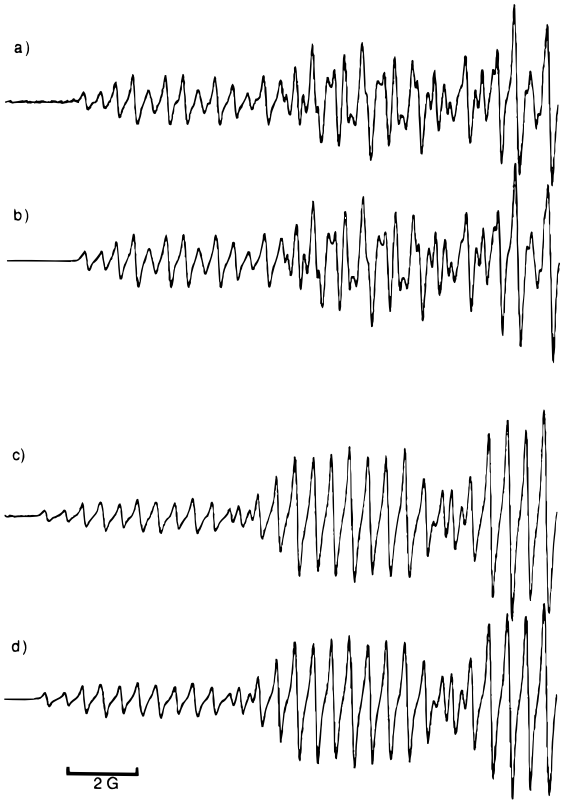

Figure 2. Low-field half of the SEEPR spectra of naphthalimide **1** radical anion: (a) experimental (10^{-3} M naphthalimide, 0.1 M TBAP, dry, degassed CH_2Cl_2); (b) simulated; (c) experimental (10^{-3} M naphthalimide, 10^{-3} M receptor **2**, 0.1 M TBAP, dry, degassed CH_2Cl_2); (d) simulated.

Addition of up to 1 equiv of receptor **2**[20] to naphthalimide radical anion **1** caused marked, progressive changes. Spectra taken at 1, 10, and 30 equiv of receptor **2** are almost identical, indicating complete complexation, a proof for the high association constant of the hydrogen bound complex. Spectra acquired at less than 1 equiv of receptor **2** are a superposition of the spectra for the bound and unbound naphthalimide radical anion **1**, indicating that the lifetime of the complex is longer than the EPR time scale ($\sim 10^{-6}$ s). Previously studied model systems[9-12] for hydrogen bound radical anions exhibited averaged hyperfine coupling constants rather than superimposed spectra at less than 100% complexation, indicating a lifetime for the complex shorter than the EPR time scale, consistent with weaker and less specific interactions. To rule out naphthalimide dimer formation, the NMR spectra of naphthalimide and EPR spectra of the naphthalimide radical anion **1** were acquired over a 10^2 concentration range; the spectra remained unaltered, indicating little imide−imide interaction.

Addition of receptor **2** to *N*(1)-methylnaphthalimide radical anion **3**, in which the binding site is blocked through alkylation, causes little change in the EPR spectrum. Upon addition of 3 equiv of receptor **2** to radical **3**, the spectrum of a second species becomes observable, amounting to 2% of the total spectrum (Figure 3). This species is most likely the result of weak, nonspecific interactions, since addition of up to 30 equiv of receptor **2** to radical **3** does not cause full conversion of the spectrum. Complex formation between naphthalimide radical anion **1** and receptor **2** on the other hand is complete after the

(16) Niemz, A.; Imbriglio, J.; Rotello, V. M. *J. Am. Chem. Soc.* **1997**, *119*, 887−892.

(17) NIEHS WinSim EPR, version 0.95: Duling, D., Laboratory of Molecular Biophysics, NIEHS, NIH, DHHS, 1994.

(18) Gaussian 94, Revision D.4: Frisch, M. J.; Trucks, G. W.; Schlegel, H. B.; Gill, P. M. W.; Johnson, B. G.; Robb, M. A.; Cheeseman, J. R.; Keith, T.; Peterson, G. A.; Montgomery, J. A.; Raghavachari, K.; Al-Laham, M. A.; Zakrzewski, V. G.; Ortiz, J. V.; Foresman, J. B.; Cioslowski, J.; Stefanov, B. B.; Nanayakkara, A.; Challacombe, M.; Peng, C. Y.; Ayala, P. Y.; Chen, W.; Wong, M. W.; Andres, J. L.; Replogle, E. S.; Gomperts, R.; Martin, R. L.; Fox, D. J.; Binkley, J. S.; Defrees, D. J.; Baker, J.; Stewart, J. P.; Head-Gordon, M.; Gonzalez, C.; Pople, J. A., Gaussian, Inc., Pittsburgh, PA, 1995.

(19) Koh, A. K.; Miller, D. J. *At. Data Nucl. Data Tables* **1985**, *33*, 235−253.

(20) Equivalents of receptor with respect to amount of naphthalimide present. Since bulk electrolysis is not exhaustive, the concentration of naphthalimide radical anion **1** is lower than the concentration of naphthalimide.

Table 1. Experimental and Calculated hfc's (G) of the Naphthalimide Radical Anion **1**

	experimental hfc's[d]			UHF 6−31G* hfc's			B3LYP 6−31G* hfc's		
atom	**1**[a]	**1**+**2**[b]	Δ[c]	**1**[a]	**1** + **2**[b]	Δ[c]	**1**[a]	**1** + **2**[b]	Δ[c]
N(1)	1.424	1.492	0.068	−4.085	−6.015	1.930	−1.152	−1.281	0.129
H(1)	0.480	0.533	0.053	3.699	0.107	−3.592	0.547	0.005	−0.542
H(3)/H(8)	5.112	5.282	0.170	−24.003	−26.235	2.232	−5.046	−5.747	0.701
H(4)/H(7)	0.908	1.028	0.120	18.644	20.849	2.205	0.992	1.520	0.528
H(5)/H(6)	5.744	5.763	0.019	−27.182	−27.860	0.678	−6.892	−7.055	0.163

[a] Naphthalimide radical anion **1** alone. [b] 1:1 complex between naphthalimide radical anion **1** and receptor **2**. [c] Difference in the absolute magnitude: $\Delta = |\text{hfc}(\mathbf{1}+\mathbf{2})| - |\text{hfc}(\mathbf{1})|$. [d] Absolute values, average dispersion approximately ±0.005 G.

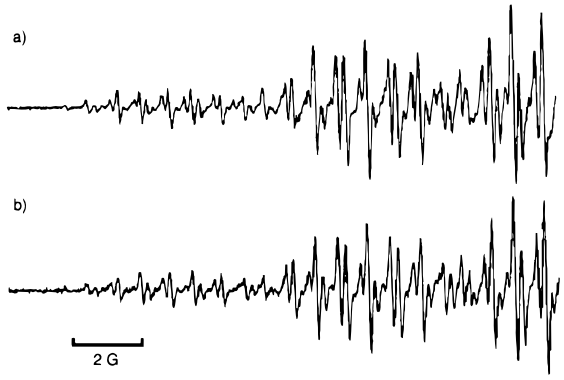

Figure 3. Low-field half of the SEEPR spectra of *N*(1)-methylnaphthalimide radical anion **3**: (a) 10^{-3} M *N*(1)-methylnaphthalimide, 0.1 M TBAP, dry, degassed CH_2Cl_2; (b) 10^{-3} M *N*(1)-methylnaphthalimide, 3×10^{-3} M receptor **2**, 0.1 M TBAP, dry, degassed CH_2Cl_2.

addition of 1 equiv of receptor **2**, confirming that the interaction is specific and based on hydrogen bonding.

To further correlate experimental results with changes in spin densities, we carried out a series of *ab initio* UHF and DFT-B3LYP calculations. It is now widely recognized that calculations based on UHF wave functions overestimate spin densities and isotropic hfc's in π-radicals.[21−23] While post-Hartree−Fock methods have been applied successfully to study small radicals, computational effort makes application to larger systems prohibitive. The B3LYP self-consistent hybrid functional has been proven especially useful for the prediction of spin density distribution and isotropic hfc's in organic π-radicals[24,25] and has been shown in several cases to accurately model hydrogen bond interactions,[26,27] and biologically relevant radicals.[23,27−29] The computational economy of density functional theory makes it the method of choice for larger systems such as the one presented here.

From the experimental values (Table 1) it is apparent that every observed hfc increases in absolute magnitude upon hydrogen bond formation. Hydrogen bonding hence leads to an increase in overall spin polarization, also manifested in an increase of spectral width. Interestingly, the largest changes are not observed at the binding site, but in the naphthalene moiety of radical **1**. These trends are well represented by both UHF and DFT computational methods. While hfc's derived from UHF calculations are on average an order of magnitude too high, the hybrid B3LYP functional-derived hfc's are in much better quantitative agreement with experimental values. The only discrepancy is the predicted decrease in the hfc of imide proton H(1). Since this hydrogen derives its spin density through secondary spin polarization from the carbonyl carbons via the imide nitrogen, and is furthermore directly involved in hydrogen bonding, calculating its spin density is especially complex. The overall increase in spin polarization upon hydrogen bonding is overestimated by the B3LYP calculations, but relative amounts of change between different sites are predicted correctly. Therefore, it can be concluded that the B3LYP hybrid density functional employing the 6-31G* basis set provides a reasonable computational method to study the effect of hydrogen bonding on the spin density distribution of naphthalimide radical **1**.

Table 2. Calculated Spin Densities (sd)

	B3LYP 6−31G* spin densities		
atom	**1**[a]	**1** + **2**[b]	Δ[c]
N(1)	−0.032	−0.040	0.008
C(2)/C(9)	0.052	0.084	0.031
O(2)/O(9)	0.083	0.079	−0.004
C(2a)/C(8a)	0.048	0.004	−0.044
C(3)/C(8)	0.203	0.236	0.033
C(4)/C(7)	−0.076	−0.099	0.023
C(5)/C(6)	0.290	0.296	0.006
C(5a)	−0.112	−0.119	0.007
C(2b)	−0.011	0.005	−0.006

[a] The naphthalimide radical anion **1**. [b] The 1:1 complex between **1** and receptor **2**. [c] Difference in the absolute magnitudes: $|\text{sd}(\mathbf{1}+\mathbf{2})| - |\text{sd}(\mathbf{1})|$.

Since experimental and calculated hfc's are in reasonable agreement, the computational results can be used to predict properties not directly accessible via simple EPR experiments, e.g., changes in spin density distribution within the π-framework upon hydrogen bonding. According to B3LYP calculations, the largest increase in the absolute value of the spin density within the π-framework (Table 2) is observed at the C(3)/C(8) and C(4)/C(7) positions of the naphthyl portion of radical **1**, and the carbonyl carbons C(2)/C(9). The spin density at the carbonyl oxygens, which are directly involved in hydrogen bonding, is actually decreased. This can be understood if one considers that hydrogen bonding is a two-electron process: lower, filled molecular orbitals are distorted toward the binding site, leading to an increase in charge density at the carbonyl oxygens. The semioccupied molecular orbital (SOMO) on the other hand is distorted away from the binding site.

In summary, we have shown that specific hydrogen bond interactions between receptor **2** and the naphthalimide radical anion **1** cause marked changes in the spin density distribution involving the entire π-system, increasing the total amount of unpaired spin by enhancing spin polarization. This provides a model for the stabilization of radical anions in biological systems, and the fine-tuning of their reactivity. Future studies will extend the combined experimental/computational approach presented here to biologically relevant systems such as flavin

(21) Chipman, D. M. *Theor. Chim. Acta* **1992**, *82*, 93−115.
(22) Cramer, C. J. *J. Org. Chem.* **1991**, *56*, 5229−5232.
(23) Qin, Y.; Wheeler, R. A. *J. Phys. Chem.* **1996**, *100*, 10554−10563.
(24) Adamo, C.; Barone, V.; Fortunelli, A. *J. Chem. Phys.* **1995**, *102*, 384−393.
(25) Barone, V. *Theor. Chim. Acta* **1995**, *91*, 113−128.
(26) Barone, V.; Orlandini, L.; Adamo, C. *Chem. Phys. Lett.* **1994**, *231*, 295−300.
(27) O'Malley, P. J.; Collins, S. J. *Chem. Phys. Lett.* **1996**, *259*, 296−300.
(28) Qin, Y.; Wheeler, R. A. *J. Chem. Phys.* **1995**, *102*, 1689−1698.
(29) Jensen, G. M.; Goodin, D. B.; Bunte, S. W. *J. Phys. Chem.* **1996**, *100*, 954−959.

and quinone cofactors, and will be reported in due course.

Acknowledgment. This research was supported by the National Science Foundation (Grant CHE-9528099) and the Petroleum Research Fund of The American Chemical Society (Grant 30199-G4). V.M.R. thanks Research Corp. for a Cottrell Fellowship. We thank Prof. Paul Lahti for helpful discussions.

Supporting Information Available: Experimental and simulated SEEPR spectra of the radical anions **1** and **3** at different concentrations and in the presence of varying amounts of receptor **2** (15 pages). See any current masthead page for ordering and Internet access instructions.

JA970801A